Environmental Toxicology and Pharmacology 109 (2024) 104477

Contents lists available at ScienceDirect

Environmental Toxicology and Pharmacology

journal homepage: www.elsevier.com/locate/etap

Biochar dust emission: Is it a health concern? Preliminary results for toxicity assessment

Silvana Pinelli [a,1], Stefano Rossi [a,1], Alessio Malcevschi [b], Michele Miragoli [a,c,d], Massimo Corradi [a,c], Luisella Selis [a], Sara Tagliaferri [a,c], Francesca Rossi [e], Delia Cavallo [f], Cinzia Lucia Ursini [f], Diana Poli [f], Paola Mozzoni [a,c,*]

[a] Department of Medicine and Surgery, University of Parma, Parma, Italy
[b] Department of Chemistry, Life Sciences and Environmental Sustainability, University of Parma, Parma, Italy
[c] Centre for Research in Toxicology (CERT), University of Parma, Parma, Italy
[d] Humanitas Clinical and Research Center, IRCCS, Rozzano, Milan, Italy
[e] National Research Council (CNR), Istituto dei Materiali per l'Elettronica ed il Magnetismo (IMEM), Parma, Italy
[f] INAIL Research, Department of Occupational and Environmental Medicine, Epidemiology and Hygiene, Monte Porzio Catone, Italy

ARTICLE INFO

Edited by M.D. Coleman

Keywords:
Biochar
Occupational exposure
Environmental pollution
In-vitro studies
In-vivo studies

ABSTRACT

Biochar is currently garnering interest as an alternative to commercial fertilizer and as a tool to counteract global warming. However, its use is increasingly drawing attention, particularly concerning the fine dust that can be developed during its manufacture, transport, and use. This work aimed to assess the toxicity of fine particulate Biochar (<PM_{10}) via *in-vitro* and *in-vivo* experiments as a first step for the evaluation of toxicity values. As *in-vitro* experiments, cell lines showed inhibition of proliferation following the reduction of expression genes involved in cell cycle control, increase in the production of ROS and IL-8, and decrease in intracellular ATP. *In-vivo* rat exposure induced hyperemia, edema, and inflammatory phenomena with infiltrations of neutrophil granulocytes and macrophages at the alveolar and bronchiolar levels. Both *in-vitro* and *in-vivo* studies highlighted how exposure to Biochar particulates leads to an inflammatory condition and oxidative stress.

1. Introduction

Biochar is a fine-grained, highly porous charcoal made from the thermal degradation of plant biomass. It is currently attracting considerable interest as a soil improver (Spokas et al., 2012) and a tool to counteract global warming (Yin et al., 2021) due to its distinctive physical/chemical/biological properties, including high water-holding capacity (Batista et al., 2018), large surface area cation exchange capacity (Munera-Echeverri et al., 2018) elemental composition (Denyes et al., 2014), and pore size/volume/distribution. These positive effects may be undermined by its possible contamination by toxic compounds formed or adsorbed during its production, which depends to a notable extent on temperature and on the kind of plant biomass used (Qiu et al., 2015). These hazardous chemicals may include primarily polycyclic aromatic hydrocarbons (PAHs), but also metals (e.g. cadmium, copper, chromium, lead, zinc, mercury, nickel, and arsenic), volatile organic cThese authors contributed equally to this workompounds (VOCs), dioxins, furans, and Polychlorinated biphenyls (PCBs) (Gelardi et al., 2019).

In this context, growing attention is being paid to characterize the chemical and physical properties of different Biochar (Campos et al., 2020; de la Rosa et al., 2014), and a regulatory framework for Biochar production, quality assurance and application is under development (The European Biochar Certificate guides MPLs in Biochar for use in soil in their accreditation system, which can be found at the following link: http://www.european-biochar.org/en). The International Biochar Initiative (IBI) has also produced voluntary guidelines for Biochar that are used in soils, which include maximum permissible limits (MPLs) for heavy metals and organic pollutants (http://www.biochar-international.org/). Nevertheless, the knowledge about the relationships between Biochar chemical and physical properties and their effects on living organisms is still scanty with most studies focused so far mainly on soil biota (He et al., 2021), whereas the effects on humans have not yet been investigated systematically. To note, chemical analyses are not a

* Correspondence to: Department of Medicine and Surgery, University of Parma, Via Gramsci 14, Parma 43126, Italy.
E-mail address: paola.mozzoni@unipr.it (P. Mozzoni).
[1] These authors contributed equally to this work

https://doi.org/10.1016/j.etap.2024.104477
Received 30 November 2023; Received in revised form 14 May 2024; Accepted 20 May 2024
Available online 27 May 2024

sufficient tool for estimating health risks associated with Biochar-induced dust exposure. It is known that when manufacturing or applying pure Biochar, fine dust may result from the collision, abrasion, grinding, and pulverization of charcoal chunks. Prolonged exposure to carbon small particles through employment, e.g. in coal mining or old-style kilns, especially where deficient workplace conditions can lead to exceed the limit levels (de la Rosa et al., 2014; Kania et al., 2014). Biochar produced by low-efficient pyrolysis plants is characterized by very low mechanical strength and high brittleness (Das et al., 2016); therefore, during the emptying of plant, shifting, reloading and transport, it undergoes considerable fragmentation. Recent studies suggest that the number of workers occupationally exposed to Biochar dust is likely to increase because of its increasing application in soil (Li et al., 2023; Wang et al., 2022; Yu et al., 2019). However, data on the health risks resulting from its production, transport and use remain very limited and mainly concern the problem of dust inhalation. It is known that breathing, dermal absorption, or ingesting particulate charcoal with a diameter of less than 10 μm (PM_{10}) poses a variety of health risks like other small particles arising from human activities (Bonalumi and Miragoli, 2023; De Donno et al., 2018).

Epidemiological studies on humans have associated exposure to high concentrations of PM_{10} (>200 mg/m^3), with increased lung diseases and cardiovascular morbidity (Chen and Hoek, 2020; Di Blasi et al., 2022). Respirable particles, producing reactive oxygen species (ROS), increase the production of mediators of pulmonary inflammation and may trigger or promote the mechanisms of pulmonary disease (e.g. endothelium inflammation, pneumoconiosis, chronic bronchitis, loss of lung function, emphysema, progressive massive fibrosis, and lung cancer) (Kania et al., 2014; Valavanidis et al., 2013). Dust inhalation-mediated cardiovascular toxicity is characterized by the activation of pro-inflammatory pathways and the generation of ROS (Gangwar et al., 2020). It has been proved that ultra-fine particles cause harm is by creating reactive oxygen species (ROS) in the heart muscle and endothelial cells (Rossi et al., 2021). This leads to various negative effects such as myocardial stunning, necrosis, vascular dysfunction, and apoptosis, which are linked to higher levels of ROS (Zorov et al., 2014). In addition, there is some evidence that small micrometer-to-nanometer-sized carbon particles may cross biological barriers, enter the bloodstream, and spread in tissues and fetal organs distant from the site of adsorption (Lu et al., 2016) affecting the entire organism with effects including changes in development and the immune response (Gour et al., 2018).

All these aspects, being a potential source of toxic compounds, or the ability to bind pollutants, highlight the need to understand whether exposure to Biochar dust is a health issue, particularly for workers.

The present work aimed to study the toxicity of fine particulate Biochar (<PM_{10}) via *in-vitro* and *in-vivo* experiments. Time and concentration-dependent effects of Biochar were evaluated *in-vitro* tests investigating multiple cell functions (e.g. cell viability, cell cycle, repression/activation of cytokines, ATP synthesis, oxidative stress, ROS production). *In-vivo* tests were conducted via Biochar intra-tracheal instillation in rats, to evaluate the effect on different tissues (e.g. inflammatory phenomena, oxidative stress, etc.) after exposure.

2. Methods

2.1. Biochar production and collection

The Biochar was collected from a biomass pyro-gasification power plant mainly intended for electricity and heat generation according to the principle of combined heat and power (CHP) as previously described (Sirico et al., 2020, 2021). Briefly, plants were located in the North of Italy (mainly broadleaf trees, such as chestnut, pine, and fir) and the woodchips, with sizes between 30 mm and 90 mm, were first dried and then transported from the storage bunker to the plant by a screw conveyor. Tar-less wood gas was then produced from biomass and various oxidation chemical reactions took place in the plant releasing the heat needed for the endothermic reactions, with the final production of syngas and carbon. The Biochar powder was characterized and used as received from the plant, without sieving or grinding reducing the environmental impacts and making the recycling process more sustainable.

2.2. Characterization of biochar fragments by electron microscopy

The charcoal was analyzed by Scanning Electron Microscopy (SEM) in a Cambridge 360 Stereoscan SEM operated at an accelerating voltage of 10 keV, allowing to resolve details above 200 nm. The statistical analysis of the size distribution of the charcoal fragments was performed using the ImageJ software [http://imagej.nih.gov/ij/] to obtain the Feret diameter (or caliper diameter). Transmission Electron Microscopy (TEM) was also performed, using a JEOL JEM 2200FS operated at 200 kV in conventional bright field or high-resolution imaging mode. The samples were prepared by drop-casting a suspension of charcoal fragments, sonicated in ethanol, on a polished silicon substrate for SEM observation or a carbon-coated copper grid for TEM analysis.

2.3. In-vitro studies

Unless otherwise specified, Merck Life Science S.r.l. (Milano, Italy) was the source of all chemicals and reagents for *in-vitro* studies.

2.3.1. Cell culture and treatment

Cell lines A549 (adenocarcinoma alveolar basal epithelial cells) and HT29 (colorectal adenocarcinoma cells), both obtained from American Type Culture Collection (Manassas, VA, USA), used in this study, were cultured in RPMI 1640 (Lonza, Verviers, Belgium), supplemented with 10 % (v/v) fetal bovine serum, penicillin (100 U/ml), streptomycin (100 μg/ml) and L-Glutamine (2 mM). Cells were maintained under standard conditions at 37°C and 5 % CO_2 in a water-saturated atmosphere and seeded at a density of 50,000cells/cm^2, then left to attach for 24 h before treatments.

Cells were treated with Biochar prepared in a cell culture medium at a final concentration of 0, 10, 50, 100, or 250 μg/ml.

During incubation with Biochar, the morphology of cells was monitored under an inverted microscope (CK40-RFL Olympus, Tokyo, Japan).

2.3.2. Cellular uptake

Cellular interaction with Biochar was studied by flow cytometry in both lines, evaluating the changes in cell parameters, as described previously (Alinovi et al., 2015; Cacchioli et al., 2014; Zucker et al., 2013). 2- to 3-mm polystyrene beads were used for calibration and alignment of the FC500™ flow cytometer (Instrumentation Laboratory, Bedford, MA, USA). Both forward scatter (FSC) and side scatter (SSC) were acquired with linear amplification, setting the dynamic ranges to show the maximum changes for the highest concentration tested and 10,000 events were counted. The FlowJo v.10 software package was utilized for the analysis (Tree Star Inc, Ashland, OR, USA).

Data are reported as "mean SSC ratio"; in detail, we evaluated the ratio between the mean of SSC values and mean of SSC of control samples (treated/control) from 30 min to 24 h after 50 μg/ml Biochar, while the dose-response curve (from 0 to 250 μg/ml) was evaluated at 24 h.

2.3.3. Cytotoxicity and cell viability

The cytotoxicity was evaluated by CytoTox-One™ assay (Promega GmbH, Germany), a homogeneous, fluorometric method for estimating the number of non-viable cells, measuring the membrane damage through lactate dehydrogenase (LDH) leakage into the surrounding culture medium.

Furthermore, the cell viability was evaluated by CellTiter-Glo Luminescent Cell Viability Assay (Promega GmbH, Germany) which is

a luminescent method to determine the number of viable cells in culture based on quantitation of the intracellular ATP content.

Relative luminescent and fluorescent units, detected with a Fluorescence microplate reader (Varian, Inc., Palo Alto, CA, USA), were expressed as relative values compared to untreated control cells.

Cell viability was also evaluated *via* the MTT (3-(4,5-dimethylthiazol-2-yl)-2,5-diphenyltetrazolium bromide) assay, as already reported (Goldoni et al., 2008). This assay is based on the cleavage of the tetrazolium salt to a formazan dye by succinate-tetrazolium reductase, which exists in the mitochondrial respiratory chain and is active only in viable cells. Cells were plated in 96-well plates. After a recovery period (24 h), increasing concentrations of Biochar were added to the medium. Three hours before the end of continuous exposure, 24 h or 48 h, MTT dye was added to each well (final concentration 0.5 % w/v) and after cell lysis, the absorbance of the formazan product was measured at 570 nm by a Spectrophotometer microwell plate reader (Multiskan Ascent Spectrophotometer, Thermo Labsystems, Helsinki, Finland). A calibration curve of untreated cells was performed. To test the possible reaction of Biochar with the probe, MTT was added to the culture media, without cells, containing different concentrations of Biochar. Data from at least 3 independent experiments were expressed as a percentage of the control. Moreover, cytotoxic test results were confirmed by the trypan blue exclusion method, counting cells in a hemocytometer.

Annexin V-FITC/propidium iodide kit was used to investigate possible apoptotic effects of Biochar, according to the manufacturer's instructions (Bender MedSystems GmbH, Vienna, Austria) and as previously described (Alinovi et al., 2015). Staurosporine (100 nM for 24 h) was used as a positive control of apoptosis.

2.3.4. Clonogenic survival assay

To assess long-term effects on cell survival a clonogenic assay was performed as previously described (Cacchioli et al., 2014; Rossi et al., 2015). Briefly, exponentially growing cells were seeded onto 6 well plates (400cells/well) and were allowed to attach for approximately 16 h, a duration shorter than the population-doubling time of the cell line. After exposure, the medium was replaced with a fresh culture medium and cells were cultured over 10 days corresponding to the time needed to obtain colonies. Cells were then fixed with methanol/acetic acid (3:1, v/v) and stained with Crystal Violet (0.5 % in methanol). Only colonies containing more than 50 viable cells were counted and survival was expressed by the ratio of the mean number of colonies in the treated condition to the mean number of colonies in the controls.

2.3.5. Cell cycle analysis

Nuclear DNA was stained with Propidium Iodide to determine the percentage of cells in different phases of the cell cycle (Alinovi et al., 2015). At least 20,000 stained cells were sorted using an FC500™ flow cytometer (Instrumentation Laboratory, Bedford, MA, USA). The analysis of cytograms was conducted using FlowJo v.10 software (Tree Star Inc, Ashland, OR, USA).

2.3.6. Oxidative stress

The cellular oxidative status was evaluated by quantifying: ROS using 2,7-dichlorodihydrofluorescein diacetate (DCFH-DA) by FC500™ flow cytometry; intracellular levels of glutathione (GSH and GSSG) using a commercial colorimetric assay (Enzo Life Sciences International Inc., Plymouth Meeting, PA) in fresh cell lysates prepared according to the manufacturer's protocol; lipid peroxidation using the thiobarbituric acid reactive substances (TBARS) (Alinovi et al., 2015); protein oxidation *via* derivatization of carbonyl groups with 2,4-dinitrophenylhydrazine (DNPH), which leads to the formation of a stable dinitrophenyl (DNP) hydrazone product, according to the previously described method (Buschini et al., 2014).

The protein concentrations, quantified by the BCA (bicinchoninic acid) Protein Assay (Thermo Scientific, Rockford, IL, USA), were used to normalize the intracellular levels of GSH and GSSG in fresh cell lysates prepared according to the manufacturer's protocol (Enzo Life Sciences, Farmingdale, NY, USA).

2.3.7. IL-8 release

To determine the pro-inflammatory impact, A549 and HT29 cells were exposed to different concentrations of Biochar. After 12 h and 24 h of incubation, the cell culture supernatants were collected and the IL-8 concentration was determined using a commercial Human IL-8 ELISA Kit (Invitrogen, Camarillo, CA, USA), according to manufacturer's instructions, and was normalized to the number of cells.

2.3.8. RNA isolation and gene expression

RNA was extracted from 10^5 cells (Trizol, Ambion, Life Technologies, CA, USA), digested with DNase I (DNA-free kit; Ambion, Life Technologies, CA, USA) to remove any genomic DNA contamination and quantified using a NanoDrop spectrophotometer (Thermo Fisher Scientific, Inc.). cDNA was synthesized using a commercial kit [High Capacity RNA to cDNA™ kit (Applied Biosystems; Thermo Fisher Scientific, Inc.)], following the manufacturer's recommended experimental conditions. RT qPCR was performed using the QuantStudio 7 Flex Real Time PCR System (Thermo Fisher Scientific, Inc.) employing TaqMan 2X Universal PCR Master Mix (Life Technologies; Thermo Fisher Scientific, Inc.) and specific primers including exon-exon junctions specifically designed for heme oxygenase- 1 (*HO-1*), superoxide dismutase- 1 (*SOD-1*), superoxide dismutase- 2 (*SOD-2*), cyclin-dependent kinase 2 (*CDK2*), cyclin-dependent kinase 4 (*CDK4*), cyclin-dependent kinase 6 (*CDK6*), cyclin-D1 (*CCND1*), cyclin E1 (*CCNE1*), and cyclin-dependent kinase inhibitor 1 A (*p21*). All assays were performed in duplicate, and one no template and two interpolate controls were used in each experiment. The expression values of each mRNA were normalized to the expression of the glyceraldehyde-3-phosphate dehydrogenase (*GAPDH*) housekeeping gene. The changes in the expression of each mRNA concerning the untreated controls were calculated using the $2^{-\Delta\Delta Cq}$ method (Livak and Schmittgen, 2001).

2.4. In-vivo studies

2.4.1. Experimental animals

Experiments were conducted on twenty 8-month-old Sprague Dawley female rats singly housed with a 12 h light cycle (lights on at 19.00 h) in a temperature-controlled room at 20–24°C with food and water available *ad libitum*. This study was realized following the recommendations in the Guide for the Care and Use of Laboratory Animals of the National Institute of Health (Bethesda, MD, USA, revised 1996), the European Guideline on Animal Experiments (Directive 2010/63/EU). The protocol was approved by the Veterinary Animal Care and Use Committee of the University of Parma (Permit: 281/2017-PR and PMS 53/2009).

2.4.2. Particle suspension

Biochar particulate matter was suspended in a physiological saline solution (10 mg/ml, stock solution). Immediately before the experiments, the suspension was vortexed and immersed in a sonication bath (Branson Ultrasonics, Danbury, CT, USA) for 5 min at 37 °C to minimize particle aggregation.

2.4.3. Intra-tracheal instillation

Animals were anesthetized intraperitoneally (i.p.) with a mixture of ketamine chloride 40 mg/kg (Imalgene, Merial, Milano, Italy) and medetomidine hydrochloride 0.15 mg/kg (Domitor, Pfizer Italia S.r.l., Latina, Italy). The instillation process was extensively described in our previous work (Savi et al., 2014). Briefly, after anaesthesia, a 16-gauge catheter was gently inserted into the trachea of rats to deliver 20 μL/100 g of body weight of saline solution (Physio) or stock solution (reaching a concentration of 2 mg/kg Biochar) utilizing a laboratory bench P200 pipette (Gilson, Dunstable, UK). Rats were divided into 4

groups:

i) Physio (N = 5): intratracheal instillation of saline solution;
ii) Biochar-acute (BA, N = 5): single intratracheal instillation of saline solution + Biochar at [2 mg/kg];
iii) Biochar-subacute (BS, N = 5): intratracheal instillation of saline solution + Biochar at [2 mg/kg] for 5 consecutively days (from Monday to Friday);
iv) Biochar-recovery (BR, N = 5): intratracheal instillation of saline solution + Biochar at [2 mg/kg] for 5 consecutively days (from Monday to Friday) and sacrificed after two days of recovery.

Administration of 0.15 mg/kg atipamezole hydrochloride (Antisedan, Pfizer, Milan, Italy) has been performed to wake up the animal. Four hours after the last instillation the animals were newly anesthetized i.p. and after euthanasia heart, lung and liver were excited, washed with PBS, and included in cryovials before freezing at −80°C.

2.4.4. Histological analysis

For histological analysis, tissue samples from liver, lung, and heart were collected. Immediately after organ removal, specimens were fixed in phosphate-buffered formalin, pH 7.4 (10 % v/v), embedded in paraffin, sliced at 5 μm and stained with hematoxylin and eosin (HE).

Slides were examined using a Nikon Eclipse E800 microscope (Nikon Corporation, Japan) with Nikon PLAN APO lenses and equipped with Camera DIGITAL SIGHT DS-Fi1 (Nikon Corporation, Japan) acquiring pictures with DS camera control unit DS-L2 (Nikon Corporation, Japan).

2.4.5. ROS-induced lipid peroxidation and inflammation in-vivo

Frozen tissue samples were homogenized and sonicated in phosphate-buffered saline supplemented with a protease inhibitor cocktail (Sigma-Aldrich, St. Louis, MO, USA). Insoluble debris was pelleted, and lipid peroxidation products were detected in the supernatants by the TBARS method, based on the condensation of malondialdehyde derived from polyunsaturated fatty acids, with two equivalents to give a fluorescent red derivative. In each sample, TBARS concentrations were normalized to total protein concentration, determined by the bicinchoninic acid Protein Assay (ThermoScientific, Rockford, IL, USA). The total measurement of protein carbonyls involves the derivatization of these groups with the DNPH. The reaction generates a hydrazone which has an absorption peak at 365 nm and a molar extinction coefficient of 22000 $M^{-1}cm^{-1}$. The tissue lysates were incubated with Streptomycin sulfate (10 % in PBS) to precipitate the DNA, centrifuged to separate the supernatant and added with 15 mM DNPH in 2.5 N hydrochloric acid for 1 hour in the dark. At the end the proteins were precipitated with 20 % (w/v) trichloroacetic acid. To remove excess DNPH, the protein pellet was then washed three times with ethanol / ethyl acetate (1:1, v-v) and finally resuspended in 8 M guanidine. Both the carbonyl content (reading at 365 nm) and the protein content (reading at 280 nm) were determined with the DU640 spectrophotometer (Beckman Coulter, Brea, CA, USA).

2.5. Statistical analysis

All experiments were performed in at least three independent trials. The statistical analysis was carried out using SPSS 17.0 software (SPSS Inc., Chicago, IL, USA). Data were analyzed through Student's t-test and two-way analysis of variance (ANOVA). The post hoc Dunnett's were employed to determine differences vs control in all *in-vitro* experiments and Tukey's tests were employed to determine differences between groups in *in-vivo* experiment. Statistical significance was set at $p<0.05$.

3. Results

3.1. Characterization of biochar

The Biochar morphology was observed by SEM (Fig. 1, top). Irregular fragments, both isolated and aggregated in clusters, were observed. As obtained by statistical analysis on the small (< 15 μm) fragments, the size distribution peaked around 1 micron. TEM was used to analyse the Biochar structure (Fig. 1, bottom), showing that the micrometric fragments are aggregates of sub-micrometric particles. The sample is mainly amorphous (Fig. 1, bottom center), but occasionally crystalline lattice fringes are observed (Fig. 1, bottom right), due to crystallites of common charcoal impurities (e.g., Si).

Chemical characterization of Biochar was reported in our previous study. Briefly, total PHAs are equal to 20.91 mg Kg^{-1} with pyrene at a higher concentration (2.14 mg Kg^{-1}, 10.2 % of the total). Zn resulted in the most abundant metal (180 mg Kg^{-1}), and Ni, Pb, Co, and Cd were also detected. Cd showed a concentration (1.56 mg Kg^{-1}) that exceeded the European guideline values (1 mg Kg^{-1}) (https://www.edqm.eu), whereas Hg was not detectable.

3.2. In-vitro experiments

When the concentration of Biochar was varied, the mean SSC ratio at 24 h exhibited a dose-dependent behavior and significant increases in both lines exposed to higher amounts of Biochar (100–250 μg/ml) (Fig. 2a). The changes in this parameter over 24 h in cells treated with 50 μg/ml are described in Fig. 2b.

From the curves it is apparent that the uptake is very fast in the first half-hour, plateauing within 1–4 hours. When HT29 and A549 cells were exposed for 24 h and 48 h to increasing concentrations of Biochar, no concentration tested elicited morphologic changes, or apoptotic or necrotic cell death, as assessed by LDH release and phosphatidylserine translocation (data not shown). However, a significant inhibition of proliferation was detected in both cultures, although A549 cells were resulted more sensitive than HT29 ones and with a dose-dependent downward trend. Proliferation was inhibited in A549 cells at 24 h starting from 100 μg/ml, while in HT29 only after 48 h of exposure at the highest Biochar concentration (250 μg/ml) (Fig. 3a-b). These effects were associated with a corresponding decrease in intracellular ATP levels (Fig. 3c). Fig. 3d is exposed to the colony-forming ability of both cell lines that were significantly affected by the treatment with the higher concentrations (100 and 250 μg/ml).

After treatment with Biochar, the analysis of the cell cycle highlighted an increase in cells in the G0/G1 phase and at the same time a decrease in their division (Fig. 4).

Detection of cyclin expression gave a precise vision into the particle-induced effects on proliferation (Fig. 5). Treatments of A549 cells for 12 hours with 100 μg/ml increased the main CDKs/cyclins (CDK4, CDK6, and CDK2) involved in checkpoint G0/G1; conversely, after 24 h cells showed a drastic decrease of the same and a significant increase of expression of p21. In HT29 cultures the main effects were observed at 24 h and only in CDK6 gene expression, significantly reduced concerning the untreated control and a significant increase of expression of p21.

Biochar was tested for its ability to induce oxidative stress in both culture cells exposed to concentrations that did not severely affect cellular metabolism (50 and 100 μg/ml). One-hour exposure to DCFH-DA-preincubated cells developed a dose-independent increase of ROS production in A549 cultures (Fig. 6a). After 30 min Biochar caused a significant increase in intracellular ROS amounts, but this early and transient effect presented a decreasing trend and did not elicit lipid peroxidation or protein oxidation, as assessed by unchanged TBARS and carbonyl groups levels (data not shown). Only a slight not significant reduction in GSH was observed (data not shown). During the entire exposure period, no evidence of oxidative stress was observed in HT29 cultures, at any concentration tested. These observations were

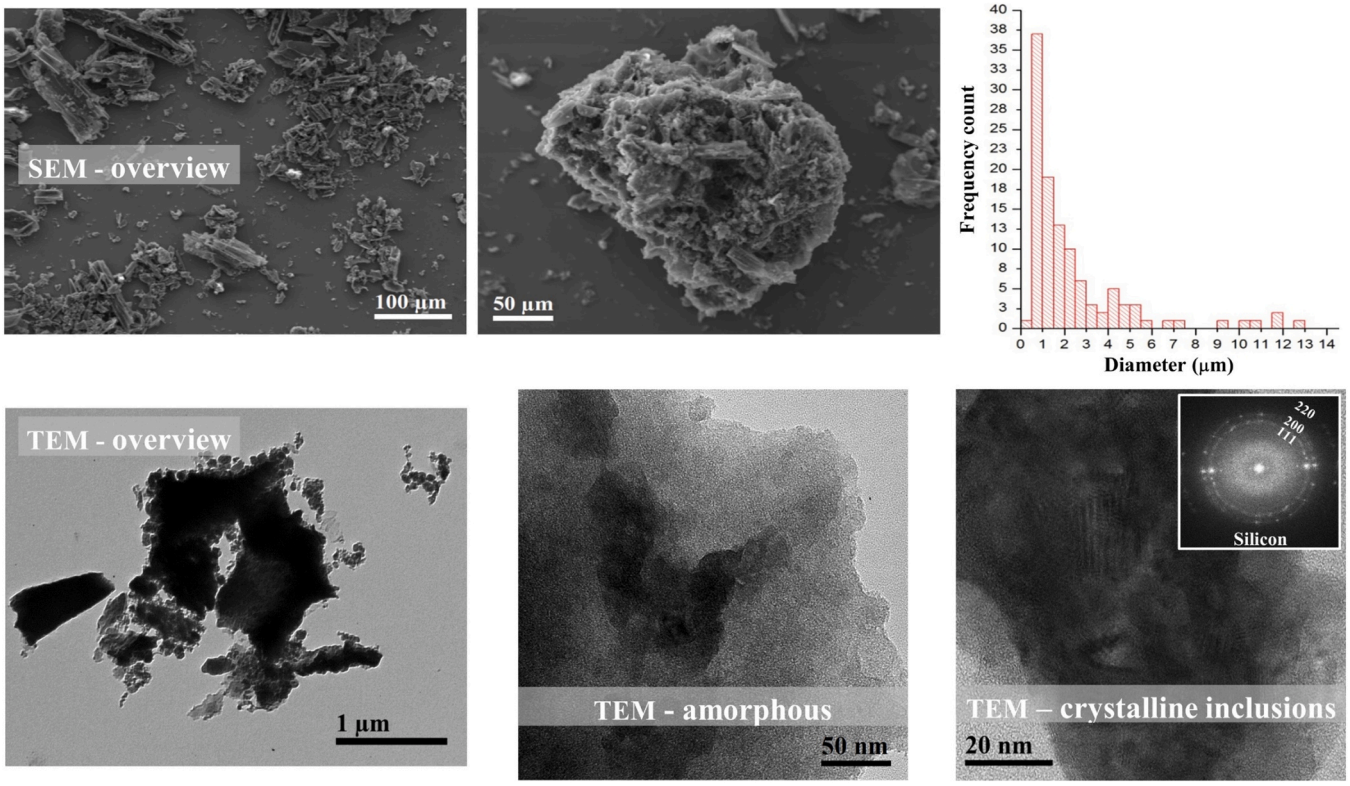

Fig. 1. Representative SEM (top row) and TEM (bottom row) images of the charcoal. Top: large area SEM image, magnified detail, and fragment size distribution. Bottom: bright-field low magnification TEM image, detail of the amorphous region, detail of crystalline inclusions (the inset shows the corresponding Fast Fourier Transform).

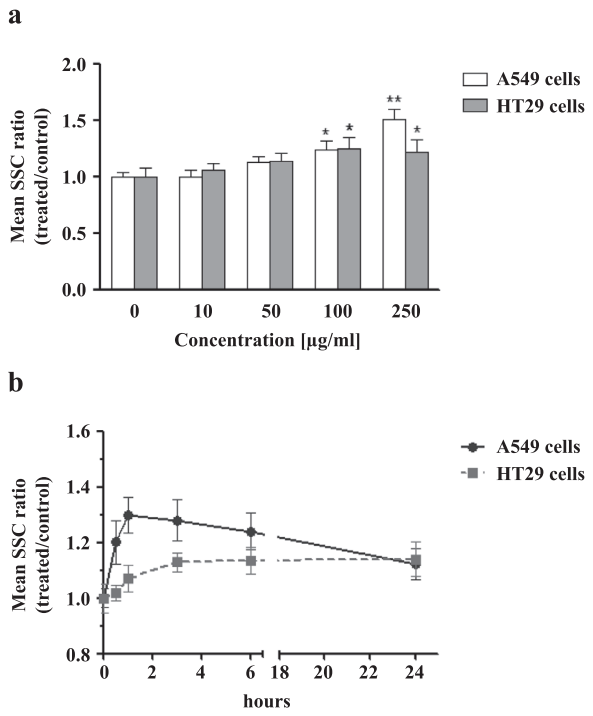

Fig. 2. Influence on side scatter (SSC) of increasing concentrations of Biochar (a) and incubation of A549 and HT29 cells with Biochar at a concentration of 50 µg/ml (b). Data are expressed as Mean SSC ratio (treated/control) ± SD. Significantly different from untreated control: *p<0.05; ** p<0.01.

corroborated by gene expression of the enzymes with antioxidant activity. Biochar-induced expression of HO-1 ($p<0.001$) and SOD-2 ($p<0.01$) only in A549 cells treated with 100 µg/ml for 12 h (Fig. 6b). This trend was followed by a decrease in both genes' expression at 24 h, thus emphasizing a cell recovery (data not shown).

Regarding the pro-inflammatory potential of Biochar, the continued treatment caused after 24 hours a dose-independent enhancement of IL-8 concentration in HT29 cells culture media but not in A549 ones (Fig. 7).

3.3. *In-vivo experiments*

The naked-eye analysis of lung tissue revealed the presence of black foci uniformly located in the parenchyma (data not shown). From the analyzes carried out on the histological preparations, it was found that, among the organs subjected to treatment with Biochar, only at the pulmonary level hyperemia edema phenomena occur and fragments of blackish material in the bronchiolar lumen were also observed (Fig. 8). In detail, we observed a slight phenomenon of hyperemia, edema and alveolar hemorrhage of focal nature in the lungs tissue in Physio group (Fig. 8a). In BA group (Fig. 8b), hyperemia, edema, and presence of fragments of blackish material (Biochar) in the bronchiolar lumen was detected, as well as an inflammatory focus with infiltrates of neutrophilic granulocytes and macrophages at the alveolar and bronchiolar level. In the BS group, a focal inflammatory phenomenon was highlighted (Fig. 8c, upper panel). Moreover, a multifocal presence of inflammatory infiltrates with alveolar and interstitial infiltration of neutrophilic granulocytes and macrophages was also observed (Fig. 8c, middle and lower panels). In the lung parenchyma of the BR group there was a focal thickening of the alveolar interstitium and an initial phenomenon of fibrosis, infiltration of macrophages that incorporate or surround particles of Biochar, with bronchus-associated lymphoid tissue hyperplasia (Fig. 8d).

From the results obtained on cardiac, liver, and lung tissue lysates it

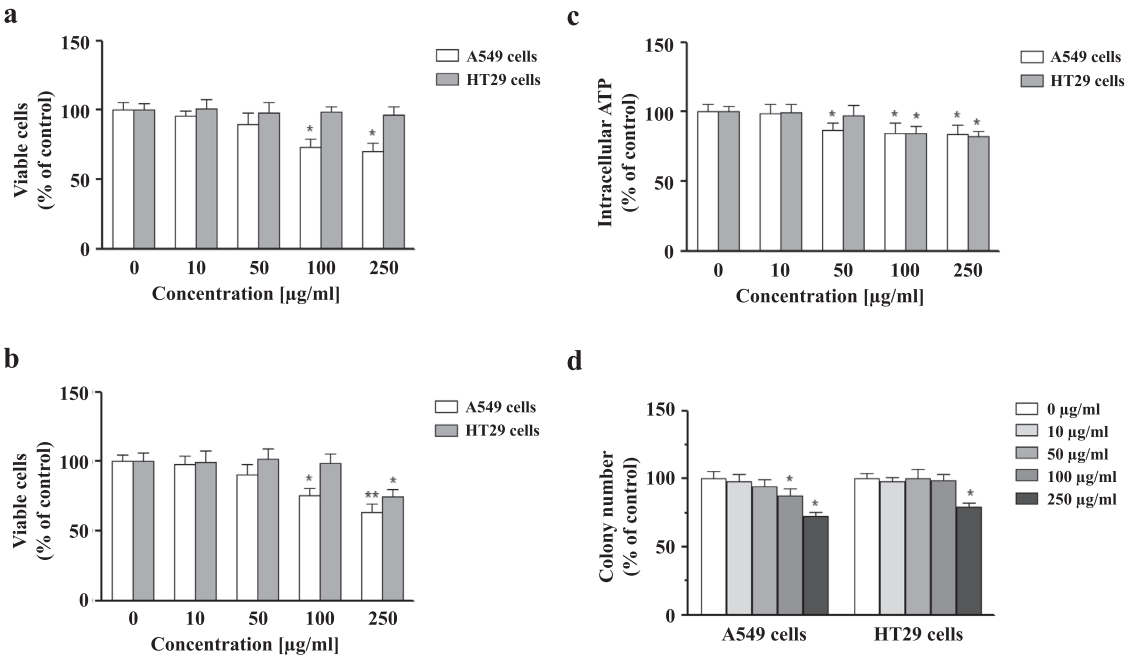

Fig. 3. Effects of Biochar on A549 and HT29 cells. Values are normalized to control. Each value represents the mean (±SD) of at least three separate experiments. *p<0.05, **p<0.01 vs control (unexposed cells). (a): viability after 24 h; (b): viability after 48 h; (c): intracellular ATP levels; (d): surviving fraction after 10 days' exposure.

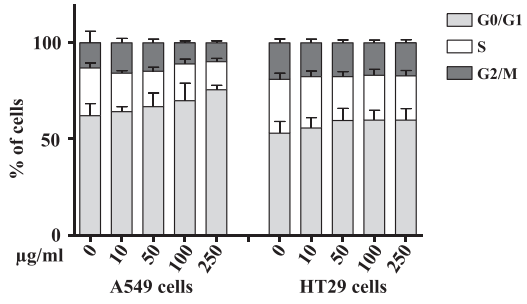

Fig. 4. Cell cycle distribution of exponentially growing cells exposed to increasing concentrations of Biochar after 24 h of treatment. By monoparametric DNA analysis three distinct phases could be recognized in proliferating cell populations, corresponding to different peaks: the G0/G1, S (DNA synthesis phase) and G2/M (mitosis).

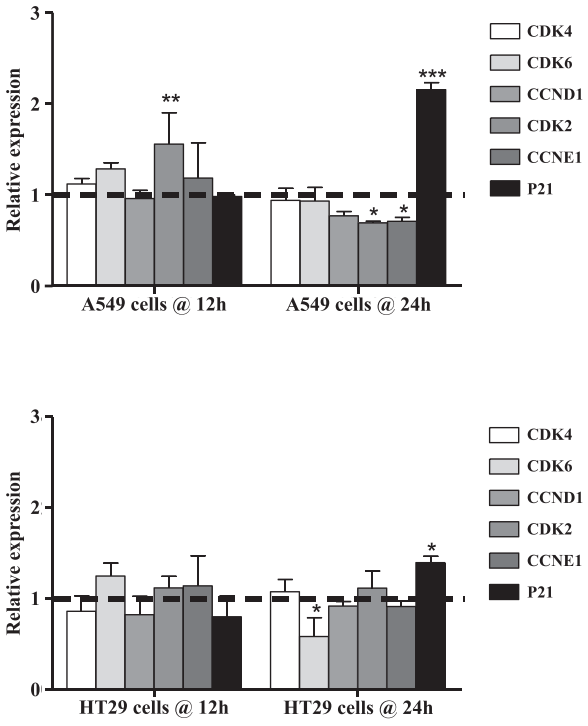

Fig. 5. Relative expression of cyclin, CDKs and P21 after 12 and 24 hours of treatment with 100 µg/ml of Biochar in A549 cells (upper panel) and HT29 cells (lower panel). *p<0.05, **p<0.01, ***p<0.001 versus control (dotted line).

can be observed that the alterations caused by Biochar on cell membranes were greater than those on proteins. The concentrations of carbonyl groups did not significantly increase in tissues after instillation compared to controls, indeed in some conditions, they even decreased (Fig. 9), although statistical significance was only achieved in the liver tissue of rats subjected to single instillation (BA). In the liver of this group of animals, lipid peroxidation is significantly increased both in comparison with controls and other treatments (Fig. 9). A non-significant increase in TBARS was also observed in the heart and lung tissues of rats that underwent Biochar tracheal instillations.

4. Discussion

Risk assessment begins with the identification of hazards and in our case, it cannot be differentiated from the physical chemical characterization of Biochar. We observed that the size distribution on the small fragments peaked around 1 micron in agreement with other works (He et al., 2018; Liu et al., 2022, 2021; Lyubov and Popova, 2017) that like us tried to establish guidelines concerning the particle sizes and the exposure level of Biochar for health effect. Furthermore, a majority of the particles were below 5µm and, thus, could easily enter the alveolar region or deep lung (Boisa et al., 2014). Biochar particles' physical and morphological properties can be significantly influenced by the feedstock and operating conditions used to produce them (Campos et al., 2020; De la Rosa et al., 2019; Mukome et al., 2013). Following what has been reported, it follows that, there are significant differences between

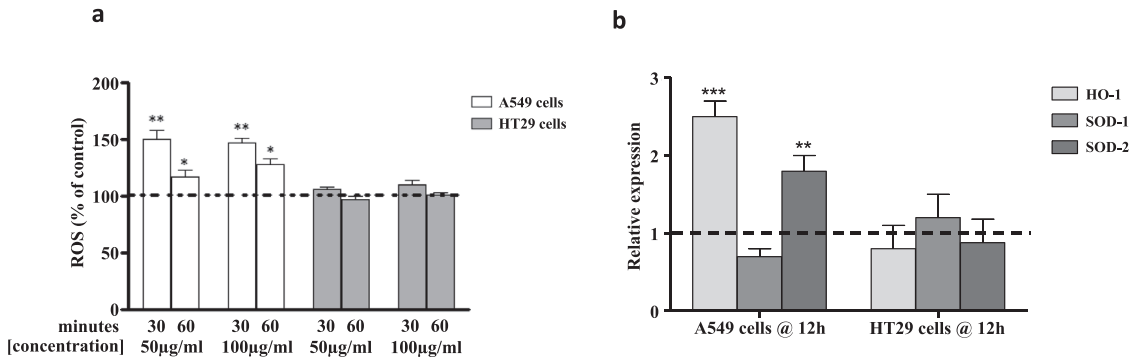

Fig. 6. Effects of biochar on ROS production (Panel a) and gene expression of HO-1, SOD-1, and SOD-2 (Panel b). Values are mean ± SD of three separate tests, each performed in triplicate. Percentage vs control = (sample value/control value) x100. Significantly different from untreated control: *p<0.05; **p<0.01: ***p<0.001.

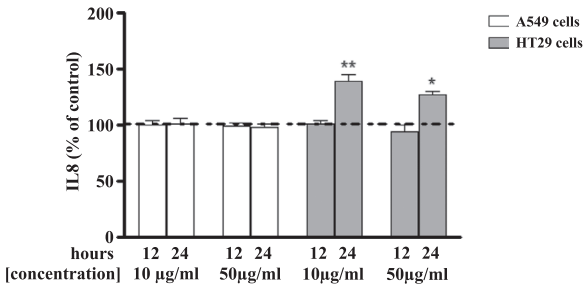

Fig. 7. Effects of Biochar on IL-8 secretion. Values are mean ± SD of three separate experiments, each carried out in triplicate. Percentage vs control = (sample value/control value) x100. Significantly different from untreated control: *p<0.05; **p<0.01.

Biochars on the market, making it impossible to compare them (He et al., 2018). While the physical size of Biochar-related PM_{10} is itself a serious concern, the organic and inorganic chemical constituents of Biochar may also present a human health risk. Biochar on the market shows no negligible concentrations of heavy metals and hazardous organic compounds, even with a slow degradation rate, which can affect both the environment and human health (De la Rosa et al., 2019; Gelardi et al., 2019). It is also interesting to note that the types and levels of heavy metals and PAHs are similar to those found in our previous work on diesel particulate matter (Rossi et al., 2021). This highlights how the main problem in Biochar management is identifying and standardizing quality chemical and physical indicators, to establish a relationship between these characteristics and potential toxicological effects.

Over the past years, a growing number of test systems for evaluating the potential toxicological hazard of xenobiotics have been developed, avoiding the use of intact animals, but founded on the use of biological

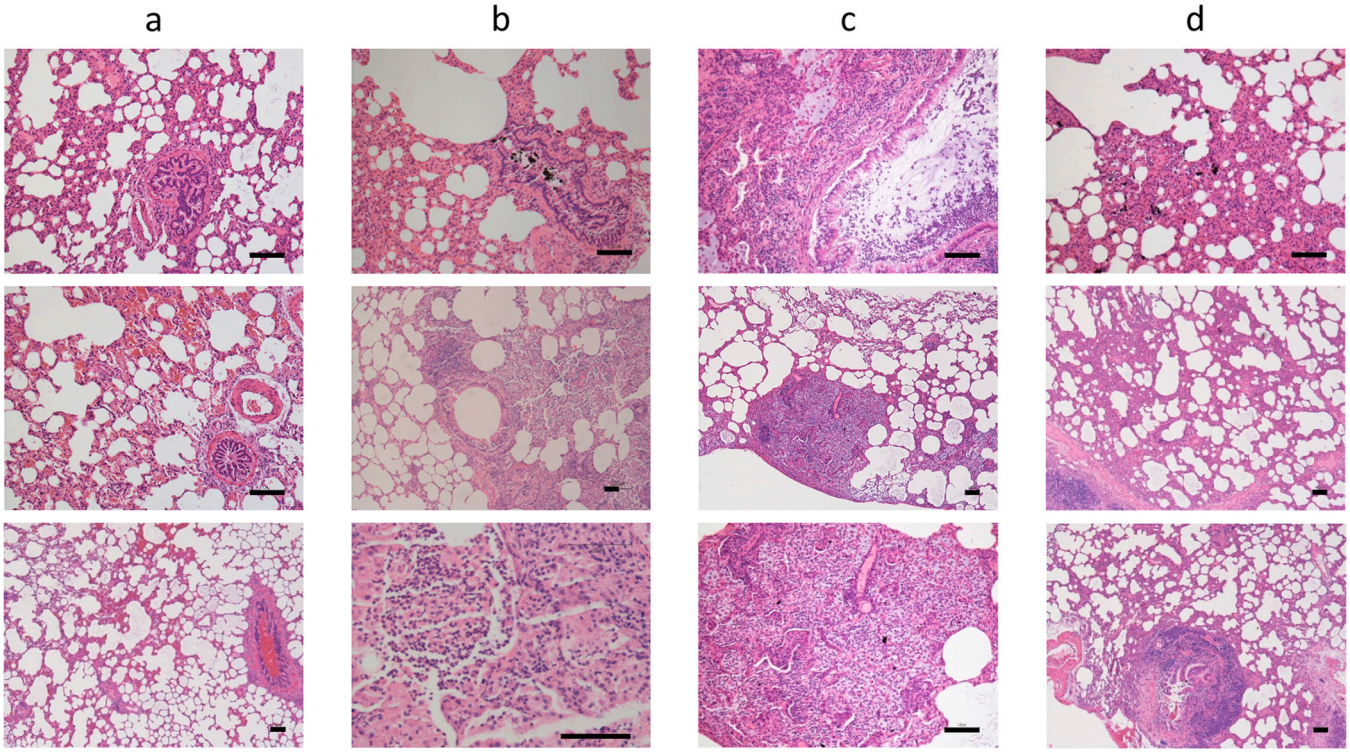

Fig. 8. Histopathologic evaluation of lung tissue stained with hematoxylin and eosin. (a) Physio group after intratracheal instillation of saline solution; (b) Biochar-acute group (BA) after a single intratracheal instillation of saline solution + Biochar at [2 mg/kg], the lower panel is a magnification of the middle panel; (c) Biochar-subacute group (BS) after intratracheal instillation of saline solution + Biochar at [2 mg/kg] for 5 consecutively days, the lower panel is a magnification of the middle panel; (d) Biochar-recovery group (BR), after intratracheal instillation of saline solution + Biochar at [2 mg/kg] for 5 consecutively days and sacrificed after two days of recovery. Scale bars in all images: 100 µm.

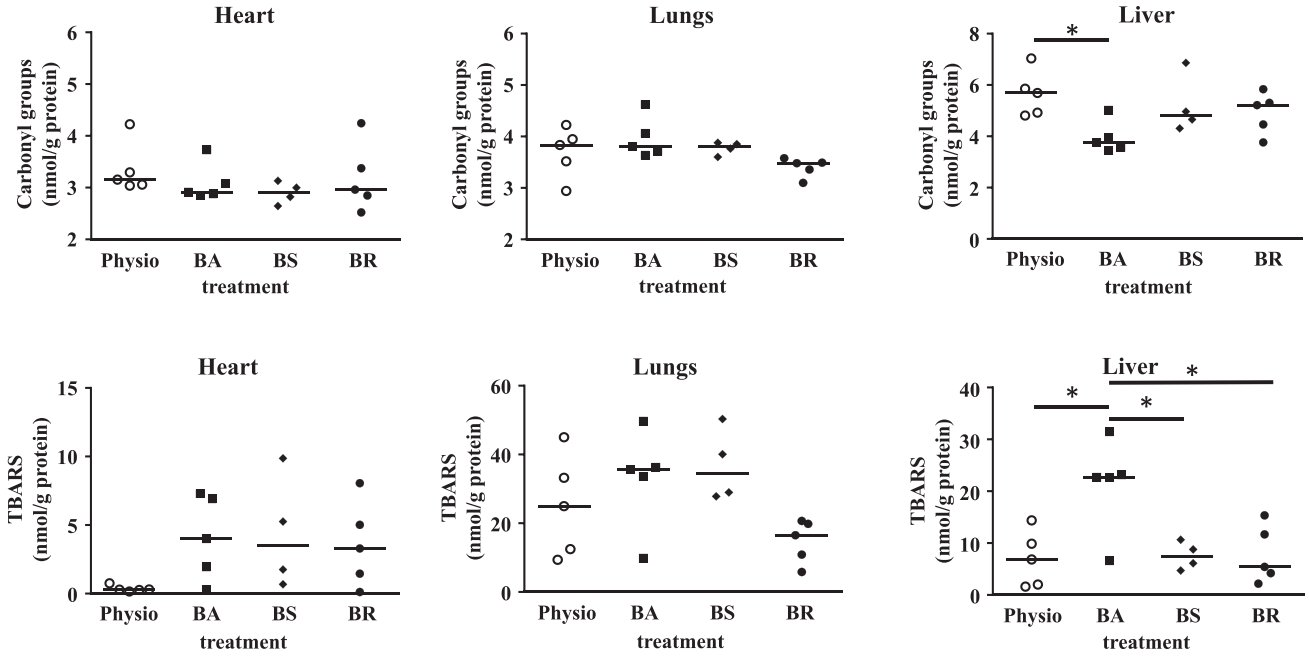

Fig. 9. Effects of Biochar on oxidative stress in the heart, lungs and liver respectively. Significantly different from untreated control: *p<0.05.

systems with a lower level of organization than the organism: isolated organs, cell cultures, and/or subcellular systems (Edler and Ittrich, 2003; Schofield, 2002). In *in-vitro* studies, concentration-effect/response curves are analysed using different mathematical models, but no reference doses other than the *EC50* have been considered. However, whereas the *EC50 in-vivo* is a parameter of systemic toxicity (50 % death), its counterpart *in-vitro* can reflect a particular toxic effect on a specific cell system. Mathematical models have been proposed to analyse *in-vitro* data and to extrapolate reference doses comparable with those observed *in-vivo* (Goldoni et al., 2003).

Both our cell lines showed a high rate of uptake during the first hour of exposure with intracellular accumulation without however showing any damage at the cellular level. Only at high doses (>100 μg/ml) was a substantial inhibition of cell viability and proliferation observed with a greater sensitivity of A549 cells compared to HT29 cells. These results agree with the work of Sigmund et al. (2017) in which a Biochar concentration of >100 μg/ml produced a marked decline in cell viability, in mouse fibroblast cell line, after incubation for 24 h and the cytotoxicity increased further after 48 h. The same trend and pattern were observed also in MRC-5 (human lung cells) cells (Yang et al., 2019). Treatment with Biochar significantly increased the percentage of cells in phase G0/G1, concomitantly with a decrease of dividing cells in both cell lines in agreement with our data on the effects of TiO_2 and Co_3O_4 nanoparticles on A549 cells (Alinovi et al., 2015).

We found that Biochar exposure is able to induce oxidative stress only in A549 cells at concentrations of 50 μg/ml and 100 μg/ml. This result is in agreement with what was obtained from de Almeida's study in which in murine fibroblasts exposed to carbon black nanoparticles there was a reduction in cell viability and proliferation, damage to cell membranes, and a rise in reactive oxygen and nitrogen species (de Almeida Rodolpho et al., 2021). More interestingly, only in HT29 cells, a rise in the pro-inflammatory potential of Biochar was evaluated by the increase in IL-8 concentration after 24 h. According to Kim et al. (2005), carbonaceous ultrafine particles seem to be a powerful inducer of proinflammatory responses in NHBE cells. As regards *in-vivo* tests, it was found that, based on histological preparations, only at the pulmonary level, Biochar treatment triggered hyperaemia edema phenomena. The analysis of histopathological samples of lung parenchyma of the experimental groups instilled with Biochar, showed mild to moderate inflammatory phenomena and a progressive thickening of the alveolar interstitium, which is a prelude to fibrosis. The irreversible structural remodelling is linked to sub-chronic exposure to Biochar which, as we have already demonstrated in the rat exposed to TiO_2-NPs, is able to induce both inflammation and upregulation of genes that promote collagen deposition and fibrosis (Rossi et al., 2019). The evaluation of TBARS and total protein carbonyls highlighted that Biochar caused oxidative stress only in liver tissue with alterations on cell membranes greater than those on proteins. More interestingly the suspension of treatments reports TBARS levels similar to control levels, as we already demonstrated in rats treated with TiO_2-NPs (Rossi et al., 2019).

Our study evaluated only acute, single exposure and evidenced that an intracellular accumulation is elicited. Even if our study did not show any severe damage at the cellular level in intestinal and lung cells, the question of the long-term effects that might occur because of chronic or recurrent inhalation of occupationally exposed workers is still unresolved. It will therefore be essential in the future to evaluate in the workplace the effects of chronic inhalation of Biochar dust, its accumulation in the lungs and the reaction of the tissues to its presence.

Typically, diseases caused by inhaling dust take many years to develop and be manifested and are characterized by a diffuse fibrotic reaction in the lungs, through the release of fibrogenic chemical mediators. Although the endpoint is fibrosis, the pattern and location vary with the type, involving activated macrophages, cytokines releases, and cell-mediated immunity resulting in granulomas (e.g. coal workers' pneumoconiosis, silicosis, asbestosis, berylliosis) (Iijima et al., 2020).

5. Conclusion

This work has highlighted the ability of Biochar to induce inflammatory and oxidative stress conditions, both *in-vitro* and *in-vivo*, whose evolution should be assessed under chronic conditions of exposure, typical of occupational settings. Recommendations from the British Biochar Foundation (https://www.biochar.ac.uk/) are appropriate ("when workers are using or applying pure Biochar, caution needs to be taken as fine dust can arise from the Biochar. There are multiple health risks associated with breathing in very small particles including respiratory diseases and even cancer. Such risks are usually associated with prolonged exposure to small particles through employment, e.g. in coal

mining, quarrying, or old-style charcoal making. However, for most Biochar applications, a simple face mask would eliminate any risk and constitutes best practice"), but so far, no Biochar exposure level has been proposed or recommended.

Further research is also needed to address knowledge gaps on the possible impact on human health as a first step in assessing and proposing a recommended level of exposure. In addition, it is crucial to investigate strategies to reduce potential damage during the production, shipment, and application of Biochar in the soil, and to define clear and unified environmental quality reference.

Ethical approval

N/A.

Funding

This research did not receive any specific grant from funding agencies in the public, commercial, or not-for-profit sectors.

Consent to participate

N/A

Consent to publish

N/A

CRediT authorship contribution statement

Sara Tagliaferri: Data curation. **Francesca Rossi:** Writing – original draft, Methodology, Investigation. **Delia Cavallo:** Writing – review & editing. **Cinzia Lucia Ursini:** Writing – review & editing. **Alessio Malcevschi:** Supervision. **Michele Miragoli:** Supervision. **Massimo Corradi:** Supervision. **Luisella Selis:** Data curation. **Paola Mozzoni:** Writing – review & editing, Methodology, Investigation, Conceptualization. **Stefano Rossi:** Writing – original draft, Methodology, Data curation, Conceptualization. **Diana Poli:** Writing – review & editing, Conceptualization. **Silvana Pinelli:** Writing – original draft, Methodology, Data curation, Conceptualization.

Declaration of Competing Interest

The authors declare that they have no known competing financial interests or personal relationships that could have appeared to influence the work reported in this paper.

Data Availability

Data will be made available on request.

Acknowledgment

A heartfelt thanks goes to Professor Anna Maria Cantoni who left us prematurely.

References

Alinovi, R., Goldoni, M., Pinelli, S., Campanini, M., Aliatis, I., Bersani, D., Lottici, P.P., Iavicoli, S., Petyx, M., Mozzoni, P., Mutti, A., 2015. Oxidative and pro-inflammatory effects of cobalt and titanium oxide nanoparticles on aortic and venous endothelial cells. Toxicol. Vitr. 29, 426–437.

Batista, E., Shultz, J., Matos, T.T.S., Fornari, M.R., Ferreira, T.M., Szpoganicz, B., de Freitas, R.A., Mangrich, A.S., 2018. Effect of surface and porosity of biochar on water holding capacity aiming indirectly at preservation of the Amazon biome. Sci. Rep. 8, 10677.

Bonalumi, F., Miragoli, M., 2023. Invited perspective: the silent threat-air pollution's Link to Arrhythmias. Environ. Health Perspect. 131, 111301.

Cacchioli, A., Ravanetti, F., Alinovi, R., Pinelli, S., Rossi, F., Negri, M., Bedogni, E., Campanini, M., Galetti, M., Goldoni, M., Lagonegro, P., Alfieri, R., Bigi, F., Salviati, G., 2014. Cytocompatibility and cellular internalization mechanisms of SiC/SiO2 nanowires. Nano Lett. 14, 4368–4375.

Campos, P., Miller, A.Z., Knicker, H., Costa-Pereira, M.F., Merino, A., De la Rosa, J.M., 2020. Chemical, physical and morphological properties of biochars produced from agricultural residues: Implications for their use as soil amendment. Waste Manag. 105, 256–267.

Chen, J., Hoek, G., 2020. Long-term exposure to PM and all-cause and cause-specific mortality: a systematic review and meta-analysis. Environ. Int 143, 105974.

Das, O., Sarmah, A.K., Bhattacharyya, D., 2016. Biocomposites from waste derived biochars: Mechanical, thermal, chemical, and morphological properties. Waste Manag. 49, 560–570.

de Almeida Rodolpho, J.M., de Godoy, K.F., Brassolatti, P., de Lima Fragelli, B.D., de Castro, C.A., Assis, M., Speglich, C., Cancino-Bernardi, J., Longo, E., de Freitas Anibal, F., 2021. Apoptosis and oxidative stress triggered by carbon black nanoparticle in the LA-9 fibroblast. Cell Physiol. Biochem 55, 364–377.

De Donno, A., De Giorgi, M., Bagordo, F., Grassi, T., Idolo, A., Serio, F., Ceretti, E., Feretti, D., Villarini, M., Moretti, M., Carducci, A., Verani, M., Bonetta, S., Pignata, C., Bonizzoni, S., Bonetti, A., Gelatti, U., Group, M.L.S., 2018. Health Risk Associated with Exposure to PM(10) and Benzene in Three Italian Towns. Int J. Environ. Res Public Health 15.

de la Rosa, J.M., Paneque, M., Miller, A.Z., Knicker, H., 2014. Relating physical and chemical properties of four different biochars and their application rate to biomass production of on a Calcic Cambisol during a pot experiment of 79 days. Sci. Total Environ. 499, 175–184.

De la Rosa, J.M., Sánchez-Martín, A.M., Campos, P., Miller, A.Z., 2019. Effect of pyrolysis conditions on the total contents of polycyclic aromatic hydrocarbons in biochars produced from organic residues: Assessment of their hazard potential. Sci. Total Environ. 667, 578–585.

Denyes, M.J., Parisien, M.A., Rutter, A., Zeeb, B.A., 2014. Physical, chemical and biological characterization of six biochars produced for the remediation of contaminated sites. J. Vis. Exp., e52183

Di Blasi, C., Renzi, M., Michelozzi, P., Donato, F.D., Scortichini, M., Davoli, M., Forastiere, F., Mannucci, P.M., Stafoggia, M., 2022. Association between air temperature, air pollution and hospital admissions for pulmonary embolism and venous thrombosis in Italy. Eur. J. Intern Med 96, 74–80.

Edler, L., Ittrich, C., 2003. Biostatistical methods for the validation of alternative methods for toxicity testing. Atla Alter. Lab Anim. 31, 5–41.

Gangwar, R.S., Bevan, G.H., Palanivel, R., Das, L., Rajagopalan, S., 2020. Oxidative stress pathways of air pollution mediated toxicity: Recent insights. Redox Biol. 34, 101545.

Gelardi, D.L., Li, C.Y., Parikh, S.J., 2019. An emerging environmental concern: biochar-induced dust emissions and their potentially toxic properties. Sci. Total Environ. 678, 813–820.

Goldoni, M., Caglieri, A., Poli, D., Vettori, M.V., Ceccatelli, S., Mutti, A., 2008. Methylmercury at low doses modulates the toxicity of PCB153 on PC12 neuronal cell line in asynchronous combination experiments. Food Chem. Toxicol. 46, 808–811.

Goldoni, M., Vettori, M.V., Alinovi, R., Caglieri, A., Ceccatelli, S., Mutti, A., 2003. Models of neurotoxicity: extrapolation of benchmark doses. Risk Anal. 23, 505–514.

Gour, N., Sudini, K., Khalil, S.M., Rule, A.M., Lees, P., Gabrielson, E., Groopman, J.D., Lajoie, S., Singh, A., 2018. Unique pulmonary immunotoxicological effects of urban PM are not recapitulated solely by carbon black, diesel exhaust or coal fly ash. Environ. Res 161, 304–313.

He, P., Liu, Y., Shao, L., Zhang, H., Lu, F., 2018. Particle size dependence of the physicochemical properties of biochar. Chemosphere 212, 385–392.

He, M., Xiong, X., Wang, L., Hou, D., Bolan, N.S., Ok, Y.S., Rinklebe, J., Tsang, D.C.W., 2021. A critical review on performance indicators for evaluating soil biota and soil health of biochar-amended soils. J. Hazard Mater. 414, 125378.

Iijima, Y., Tateishi, T., Tsuchiya, K., Sumi, Y., Akashi, T., Miyazaki, Y., 2020. Pneumoconiosis caused by inhalation of metallic titanium grindings. Intern. Med 59, 425–428.

Kania, N., Setiawan, B., Widjadjanto, E., Nurdiana, N., Widodo, M.A., Kusuma, H.M.S.C., 2014. Subchronic inhalation of coal dust particulate matter 10 induces bronchoalveolar hyperplasia and decreases MUC5AC expression in male Wistar rats. Exp. Toxicol. Pathol. 66, 383–389.

Kim, Y.M., Reed, W., Lenz, A.G., Jaspers, I., Silbajoris, R., Nick, H.S., Samet, J.M., 2005. Ultrafine carbon particles induce interleukin-8 gene transcription and p38 MAPK activation in normal human bronchial epithelial cells. Am. J. Physiol. Lung C. 288, L432–L441.

Li, Y., Gupta, R., Zhang, Q., You, S., 2023. Review of biochar production via crop residue pyrolysis: development and perspectives. Bioresour. Technol. 369, 128423.

Liu, X.L., Ma, J., Ji, R., Wang, S.F., Zhang, Q.R., Zhang, C.D., Liu, S.J., Chen, W., 2021. Biochar fine particles enhance uptake of benzo(a)pyrene to macrophages and epithelial cells via different mechanisms. Environ. Sci. Tech. Let. 8, 218–223.

Liu, B.L., Tang, C.Y., Zhao, Y., Cheng, K., Yang, F., 2022. Toxicological effect assessment of aged biochar on. J. Hazard. Mater. 436.

Livak, K.J., Schmittgen, T.D., 2001. Analysis of relative gene expression data using real-time quantitative PCR and the 2(-Delta Delta C(T)) Method. Methods 25, 402–408.

Lu, S.S., Guo, S.S., Xu, P.X., Li, X.R., Zhao, Y.M., Gu, W., Xue, M., 2016. Hydrothermal synthesis of nitrogen-doped carbon dots with real-time live-cell imaging and blood-brain barrier penetration capabilities. Int J. Nanomed. 11, 6325–6336.

Lyubov, V.K., Popova, E.I., 2017. Drying and heat decomposition of biomass during the production of biochar. J. Phys. Conf. Ser. 891.

Mukome, F.N.D., Zhang, X.M., Silva, L.C.R., Six, J., Parikh, S.J., 2013. Use of chemical and physical characteristics to investigate trends in biochar feedstocks. J. Agr. Food Chem. 61, 2196–2204.

Munera-Echeverri, J.L., Martinsen, V., Strand, L.T., Zivanovic, V., Cornelissen, G., Mulder, J., 2018. Cation exchange capacity of biochar: an urgent method modification. Sci. Total Environ. 642, 190–197.

Qiu, M.Y., Sun, K., Jin, J., Han, L.F., Sun, H.R., Zhao, Y., Xia, X.H., Wu, F.C., Xing, B.S., 2015. Metal/metalloid elements and polycyclic aromatic hydrocarbon in various biochars: the effect of feedstock, temperature, minerals, and properties. Environ. Pollut. 206, 298–305.

Rossi, F., Bedogni, E., Bigi, F., Rimoldi, T., Cristofolini, L., Pinelli, S., Alinovi, R., Negri, M., Dhanabalan, S.C., Attolini, G., Fabbri, F., Goldoni, M., Mutti, A., Benecchi, G., Ghetti, C., Iannotta, S., Salviati, G., 2015. Porphyrin conjugated SiC/SiOx nanowires for X-ray-excited photodynamic therapy. Sci Rep. 5, 7606. https://doi.org/10.1038/srep07606. Jan 5.

Rossi, S., Buccarello, A., Caffarra Malvezzi, C., Pinelli, S., Alinovi, R., Guerrero Gerboles, A., Rozzi, G., Leonardi, F., Bollati, V., De Palma, G., Lagonegro, P., Rossi, F., Lottici, P.P., Poli, D., Statello, R., Macchi, E., Miragoli, M., 2021. Exposure to nanoparticles derived from diesel particulate filter equipped engine increases vulnerability to arrhythmia in rat hearts. Environ. Pollut. 284, 117163.

Rossi, S., Savi, M., Mazzola, M., Pinelli, S., Alinovi, R., Gennaccaro, L., Pagliaro, A., Meraviglia, V., Galetti, M., Lozano-Garcia, O., Rossini, A., Frati, C., Falco, A., Quaini, F., Bocchi, L., Stilli, D., Lucas, S., Goldoni, M., Macchi, E., Mutti, A., Miragoli, M., 2019. Subchronic exposure to titanium dioxide nanoparticles modifies cardiac structure and performance in spontaneously hypertensive rats. Part Fibre Toxicol. 16.

Schofield, T., 2002. In vitro versus in vivo concordance: a case study of the replacement of an animal potency test with an immunochemical assay. Dev. Biol. (Basel) 111, 299–304.

Sigmund, G., Huber, D., Bucheli, T.D., Baumann, M., Borth, N., Guebitz, G.M., Hofmann, T., 2017. Cytotoxicity of biochar: a workplace safety concern? Environ. Sci. Tech. Let. 4, 362–366.

Sirico, A., Bernardi, P., Belletti, B., Malcevschi, A., Dalcanale, E., Domenichelli, I., Fornoni, P., Moretti, E., 2020. Mechanical characterization of cement-based materials containing biochar from gasification. Constr. Build. Mater. 246.

Sirico, A., Bernardi, P., Sciancalepore, C., Vecchi, F., Malcevschi, A., Belletti, B., Milanese, D., 2021. Biochar from wood waste as additive for structural concrete. Constr. Build. Mater. 303.

Spokas, K.A., Cantrell, K.B., Novak, J.M., Archer, D.W., Ippolito, J.A., Collins, H.P., Boateng, A.A., Lima, I.M., Lamb, M.C., McAloon, A.J., Lentz, R.D., Nichols, K.A., 2012. Biochar: a synthesis of its agronomic impact beyond carbon sequestration. J. Environ. Qual. 41, 973–989.

Valavanidis, A., Vlachogianni, T., Fiotakis, K., Loridas, S., 2013. Pulmonary oxidative stress, inflammation and cancer: respirable particulate matter, fibrous dusts and ozone as major causes of lung carcinogenesis through reactive oxygen species mechanisms. Int J. Env Res Pub He 10, 3886–3907.

Wang, C.Q., Luo, D., Zhang, X., Huang, R., Cao, Y.J., Liu, G.G., Zhang, Y.S., Wang, H., 2022. Biochar-based slow-release of fertilizers for sustainable agriculture: a mini review. Environ. Sci. Ecotech 10.

Yang, X., Ng, W., Wong, B.S.E., Baeg, G.H., Wang, C.H., Ok, Y.S., 2019. Characterization and ecotoxicological investigation of biochar produced via slow pyrolysis: effect of feedstock composition and pyrolysis conditions. J. Hazard. Mater. 365, 178–185.

Yin, X.L., Peñuelas, J., Sardans, J., Xu, X.P., Chen, Y.Y., Fang, Y.Y., Wu, L.Q., Singh, B.P., Tavakkoli, E., Wang, W.Q., 2021. Effects of nitrogen-enriched biochar on rice growth and yield, iron dynamics, and soil carbon storage and emissions: a tool to improve sustainable rice cultivation. Environ. Pollut. 287.

Yu, H.W., Zou, W.X., Chen, J.J., Chen, H., Yu, Z.B., Huang, J., Tang, H.R., Wei, X.Y., Gao, B., 2019. Biochar amendment improves crop production in problem soils: a review. J. Environ. Manag. 232, 8–21.

Zorov, D.B., Juhaszova, M., Sollott, S.J., 2014. Mitochondrial Reactive Oxygen Species (Ros) and ros-induced ros release. Physiol. Rev. 94, 909–950.

Zucker, R.M., Daniel, K.M., Massaro, E.J., Karafas, S.J., Degn, L.L., Boyes, W.K., 2013. Detection of silver nanoparticles in cells by flow cytometry using light scatter and far-red fluorescence. Cytom. Part A 83, 962–972.